

# Beam Based Alignment of Sector-1 of the SLC Linac\*

P. Emma  
 Stanford Linear Accelerator Center  
 Stanford, California 94305

## ABSTRACT

A technique is described which uses the beam to simultaneously measure quadrupole magnet and beam position monitor (BPM) transverse misalignments. The technique is applied to sector-1 of the SLC linac where simultaneous acceleration of electron and positron beams with minimal steering elements and BPMs makes quadrupole alignment critical for high transmission of the large transverse emittance positron beam. Simulation results as well as measurements are presented.

## I. INTRODUCTION

Sector-1 of the SLC linac is a ~100 meter beam line segment which accelerates electrons and positrons from 200 MeV to 1.15 GeV for injection into the damping rings. The largest section is a 60 meter dense system of 62 quadrupoles wrapped around five 40-foot rf wave guide sections to form a strong focusing FODO array designed to minimize beam size for optimal positron transmission (Fig 1). The limited space allows for only one BPM, one horizontal, and one vertical, steering corrector per wave guide. Simultaneous steering of the two beams to optimize transmission is a difficult task which has historically produced a peak e<sup>+</sup> transmission of ~90%. Optical survey alignment techniques have not routinely achieved the 100 μm rms quadrupole alignment desired and beam-based alignment techniques have worked well at the SLC [1], so the same was sought for sector-1.

## II. DESCRIPTION OF THE CONCEPT

Quadrupole and BPM transverse misalignments are calculated by assuming the linear optics between all beam line elements are known then acquiring enough non-degenerate data to construct a linear least squares fit for the unknown

misalignments. A simplified illustration of the concept is shown in Fig 2.

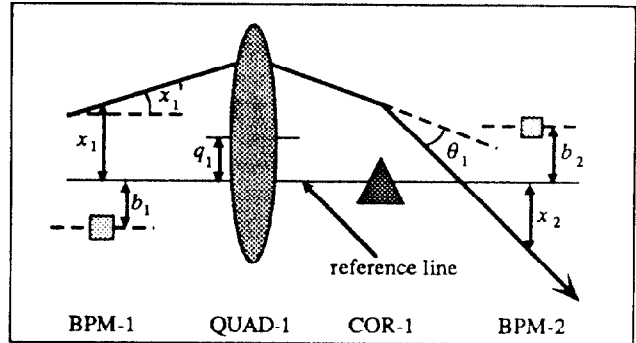


Fig 2. Simplified illustration of beam based alignment scheme

All transverse position offsets are taken with respect to an arbitrary reference line which, in practice, may be defined as (for example) a line through the first and last BPMs in the beam line. The beam position measurement ( $m_i$ ) at BPM- $i$  is assumed to be the sum of all upstream beam line kicks from quad offsets, steering correctors, incoming launch conditions, and BPM offset as in (1)

$$m_i = x_i - b_i = \begin{pmatrix} \vec{x}_i \end{pmatrix}_1 - b_i$$

$$\vec{x}_i = \mathbf{R}^{(B_1:i)} \vec{x}_1 + \sum_j^{N_{C_i}} \mathbf{R}^{(C_j:i)} \vec{c}_j + \sum_j^{N_{Q_i}} \mathbf{R}^{(Q_j:i)} (\mathbf{I} - \mathbf{R}^{(Q_j)}) \vec{q}_j \quad (1)$$

where  $b_i$  is the static offset at BPM- $i$ ,  $\mathbf{R}$  is the 2x2 transfer matrix from BPM-1 ( $B_1:i$ ), or from corrector- $j$  ( $C_j:i$ ), or from quad- $j$  ( $Q_j:i$ ), to BPM- $i$ , or simply the matrix across quad- $j$  ( $Q_j$ ).  $x_1$ ,  $c_j$  and  $q_j$  are, respectively, the incoming launch position/angle vector at BPM-1 (the first BPM in the beam line), a corrector kick angle vector, and a quadrupole position offset vector defined as

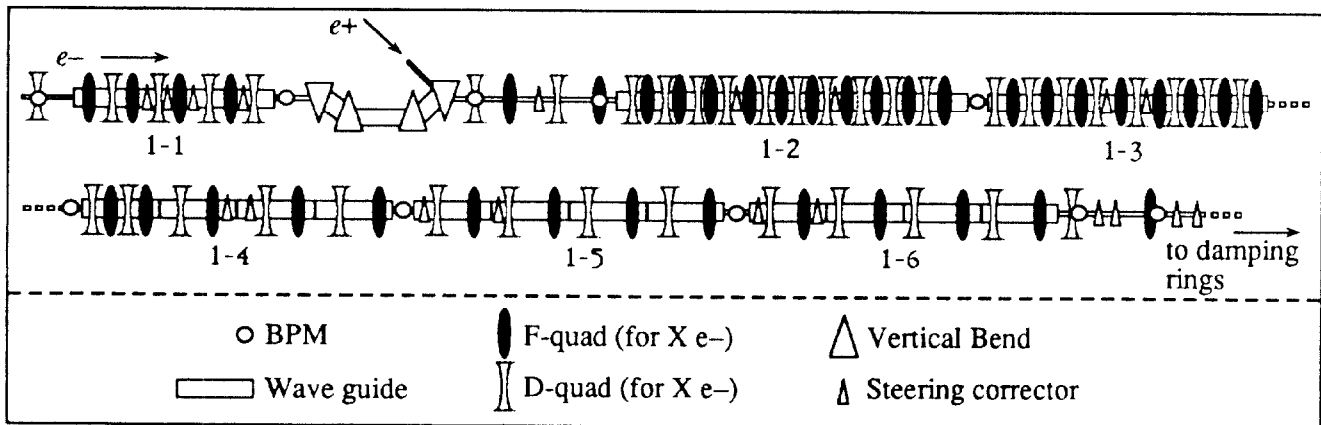


Fig 1. SLC sector-1 lattice

\* Work supported by Dept of Energy, contract DE-AC03-76FS00515

$$\vec{x}_1 \equiv \begin{pmatrix} x_1 \\ x_1' \end{pmatrix}; \quad \vec{c}_j \equiv \begin{pmatrix} 0 \\ \theta_j \end{pmatrix}; \quad \vec{q}_j \equiv \begin{pmatrix} q_j \\ 0 \end{pmatrix}. \quad (2)$$

$N_{Ci}$  and  $N_{Qi}$  are the number of correctors and quadrupoles upstream of BPM- $i$ , and  $I$  is the  $2 \times 2$  unity matrix which derives from a thick-lens quadrupole kick. The quad offset is described as only a displacement of the quad center without an attempt to resolve quadrupole pitch. This (1) is written for the horizontal plane with no X-Y coupling included (although its inclusion, when necessary, is a straight forward modification). Accordingly (1) may be written for each of the BPMs in the beam line and then this set of equations written again for a new trajectory with different quadrupole strength settings and different incoming launch conditions (to accommodate for upstream launch variations). In this way a matrix equation (per plane) is constructed from  $N_B$  BPMs,  $N_Q$  quadrupoles, and  $N_t$  different beam trajectories. The correctors are assumed to have known calibrations, however a scale factor per corrector may also be included in the fit if necessary. There are  $N_u$  unknowns (per plane) corresponding to  $N_B$  BPM offsets,  $N_Q$  quadrupole position offsets, and 2 incoming launch parameters per trajectory (also subtracting the 2 arbitrary reference line parameters)

$$N_u = N_B + N_Q + 2N_t - 2, \quad (3)$$

and  $N_m$  total measurements

$$N_m = N_B \cdot N_t. \quad (4)$$

The minimum number of different trajectories needed to uniquely solve the system is

$$N_m - N_u \geq 0 \quad \Rightarrow \quad N_t \geq \frac{N_B + N_Q - 2}{N_B - 2}. \quad (5)$$

However, to disentangle quadrupole offsets from BPM offsets requires changing the strength of each quadrupole at least once. For any quad with no strength variation its offset cannot be resolved and the static kick imparted by its offset will only arise as additional offsets to the BPMs downstream of that quad (*i.e.*, redefine the reference line coordinate system).

Stability of the linear system is a function of the difference in quadrupole strengths from one trajectory to the next and the betatron phase placement of the BPMs. This question is addressed in simulations of the particular application. The quadrupole strength changes can be implemented by rescaling (or switching off) one, several, or all quadrupoles per trajectory.

### III. SIMULATION RESULTS

Feasibility studies as well as software testing was conducted in simulation by generating many trajectories based on the sector-1 lattice with random quadrupole and BPM misalignments as well as realistic random variations in the upstream launch conditions. In addition, quadrupole focusing strength ( $k$ ) errors and BPM readback noise was introduced to examine stability of the linear system. In addition, a practical scheme for variation of the quad strengths per trajectory was

arrived at by calculating the  $\beta$  functions at all beam line elements per trajectory. By turning off adjacent pairs of quads (an FD or DF pair) the transverse rms beam size never exceeds twice the nominal value anywhere within sector-1. This scheme produces 62 trajectories ( $N_t = 62$ : one for all quads turned on and 61 with one unique adjacent pair of the 62 quads turned off —  $N_B = 8, N_u = 192, N_m = 496, DOF = 304$ ).

The beam line section chosen includes the first 8 BPMs after the  $e^+$  injection point and only those 62 quads (QW's) wrapped around the rf wave guide sections of girders 1-2 through 1-6 (fig 1). The other quads were assumed to have zero offset. This assumption only changes the definition of the reference line. No alignment was attempted upstream of the  $e^+$  injection point, and only trajectories of the electron beam were used because of its small transverse emittance compared to the positrons. Furthermore, the rf was switched off in girders 1-2 through 1-6 to produce a 200 MeV constant energy electron beam and the quadrupole strengths were rescaled such that focal lengths were that of the accelerated beam. This removed the uncertainty of the exact energy profile through the beam line.

Fig 3 shows simulation results for calculation of the horizontal quadrupole offsets given the simulation input conditions listed in Table 1 below. Error bars in fig 3 are statistical errors from the fit results using 50  $\mu\text{m}$  BPM resolution, equal for all BPMs.

BPM rms offsets	200 $\mu\text{m}$
Quad rms offsets	200 $\mu\text{m}$
BPM rms readback noise	50 $\mu\text{m}$
Quad rms $k$ errors	1%
$x_1$ launch rms variation	200 $\mu\text{m}$
$x_1'$ launch rms variation	200 $\mu\text{rad}$

Table 1. Simulation input conditions for fig 3 and 4 (all random distributions are gaussian with  $6\sigma$  cutoff).

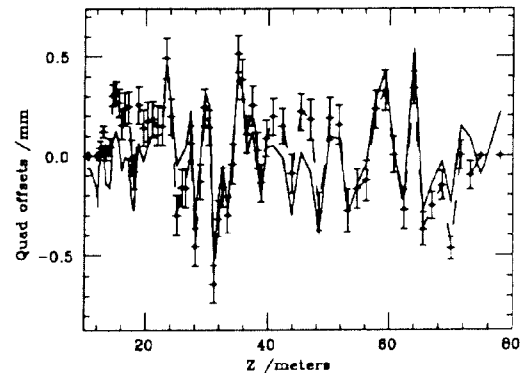


Fig 3. Quadrupole horizontal position offsets resulting from simulation conditions of Table 1. The true offsets (solid) and the fitted offsets (dashed) are shown and agree at frequencies  $> f_\beta$ .

The fitted launch conditions (not shown) also agree well with the known simulation input conditions, however these accurate fit results are only achieved by a 'chi-squared'

minimization which forces a 'soft constraint' of the fitted parameters around zero as in (6).

$$\chi^2 = \sum_{i=1}^{N_m} \frac{1}{\sigma_i^2} \left( m_i - \sum_{j=1}^{N_u} a_{ij} p_j \right)^2 + \sum_{j=1}^{N_u} \frac{1}{\delta_j^2} (p_j - c_j)^2 \quad (6)$$

Here the  $N_u$  fitted parameters,  $p_i$ , are varied to minimize not only the weighted differences to the  $N_m$  measurements,  $m_i$ , but also to minimize, within the soft constraint value of  $\delta_j$ , their differences to the constrained values  $c_j$  ( $=0$  in this application). This is necessary because this alignment method is not sensitive to low frequency ( $< f\beta$ ) variations of the quad offsets. A beam tends to smoothly focus to quad offsets that occur at frequencies lower than approximately the betatron frequency, and therefore the kick produced by switching on or off the quad is small. Small measurement errors conspire to cause an anomalous low frequency variation in the fit results. This is seen in the horizontal quad offsets of fig 4 which were fitted with the same simulation conditions of Table-1, and no 'soft constraints' applied.

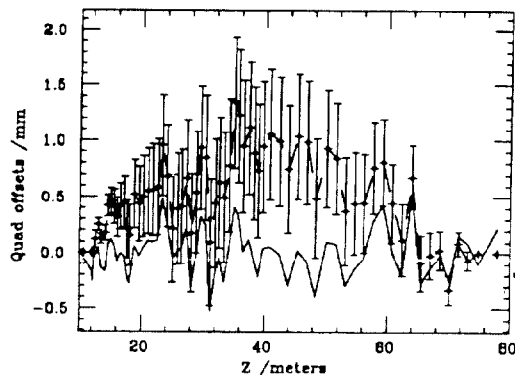


Fig 4. Same data as fig 3 with no soft constraints applied (i.e.,  $\delta_j = \infty$ ). The low frequency component drifts  $\sim 1$  mm off the true curve, however the high frequency character is still reproduced.

BPM offsets (not shown), however, are more difficult to measure accurately since their betatron spacing is  $< f\beta$ . The soft constraint values,  $\delta_j$ , used in the fit of figs 3,4 are about 2-3 times the input rms values used. These are estimated in real applications by relating the rms of a measured beam trajectory to expected quadrupole rms misalignments.

#### IV. BEAM DATA RESULTS

Data acquisition was performed with on-line software to gather the 62 quadrupole strength settings, 13 corrector settings, 8 X-BPM and 8 Y-BPM read backs, along with beam intensity readings for each of the 62 beam trajectories. The intensity is limited to  $1 \times 10^{10}$  to limit transverse wakefields.

The first trajectory is taken with all quads on. Each trajectory thereafter is taken with two adjacent quads turned off (one F-quad & one D-quad). The pair of quads to be switched off is stepped down the beam line by one quad per trajectory. After a pair is turned off the trajectory is quickly corrected by hand using the correctors to rough steer within  $\sim 1$ mm. This limits beam loss, wakefields, and BPM nonlinearities. The

corrector settings are then used in the calculation (1). Fig 5 shows fitted horizontal quad misalignments for two data sets. Fig 5a is taken before any quad moves were made while fig 5b is taken after 13 quads were moved horizontally based on the data of fig 5a (vertical alignment corrections not shown).

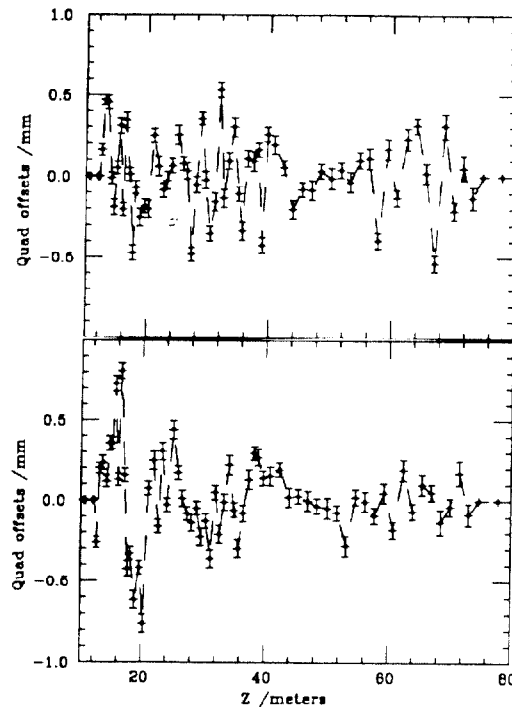


Fig 5. Horizontal measured quad offsets before (a) and after (b) tunnel corrections were made based on (a). The first 20 quads ( $Z=10$  to 30 m) have never measured reproducibly.

The large misalignment flyers ( $> 300 \mu\text{m}$ ) past girder 1-2 (fig 1) were removed. However the 20 quadrupoles on girder 1-2 have never been measured reproducibly. The reasons are not known, except to comment that this is the most dense quad section and the three BPMs in front of girder 1-2, 1-3, and 1-4 are approximately  $n\pi$  apart in betatron phase and therefore blind to some upstream quad offsets. Systematics tend to dominate in this area.

The peak positron transmission after alignment was not significantly improved. However, the necessary tune-up time for attaining good transmission was decreased and the total rms of the corrector strengths used in the region was significantly reduced making beam line setup more reproducible.

#### V. ACKNOWLEDGMENTS

I thank Chris Adolphsen and Yu Chiu Chao for many helpful suggestions including the implementation of 'soft constraints'. I also thank Torsten Limberg, Bob Siemann, and Patrick Krejcik for encouraging support and the SLC operations staff for help with data acquisition.

#### VI. REFERENCES

- [1] C.E. Adolphsen *et al*, *Beam-Based Alignment Technique for the SLC Linac* (SLAC-PUB-4902, March 1989)